MODELLING OF THE STRATOSPHERE WITH THE ECHAM GENERAL CIRCULATION MODEL

Elisa Manzini
Max-Planck-Institut für Meteorologie
Hamburg, Germany

Abstract

The large scale stratospheric circulation of a comprehensive atmospheric model is examined. The two-year simulation analyzed in the present work employed monthly climatological forcing. Successful aspects of the simulation include a clear separation between the tropospheric and stratospheric jets, the structure of the stationary planetary waves, and the suggestion of late winter interannual variability at 10 hPa in the northern hemisphere. However, the occurrence in both the northern and southern hemispheres of an overly pronounced polar temperature minimum in the winter lower stratosphere, a slightly too weak polar temperature maximum at the summer stratopause, and the virtual absence of the Quasi Biennial Oscillation in zonal wind in the equatorial lower stratosphere appear to be model deficiencies.

Results from annual mean integrations concerning the sensitivity to vertical resolution and to the location of the model top level are also presented. A warming in the polar lower stratosphere and a weakening of the stratospheric westerly wind jet were found when the model top level is moved from 10 hPa to the middle mesosphere.

1 INTRODUCTION

The study of the natural variability of the present climate and the investigation of the impact of changes in greenhouse gases and stratospheric ozone on the future climate require the development of reliable comprehensive atmospheric models eventually coupled to ocean, chemical, and biosphere models. Prior to such complex numerical simulations it is important to establish a robust confidence in the basic performance of such models. Given the multitude of the physical and dynamical processes that must be included in a comprehensive atmospheric model, to achieve such a confidence is a challenging task that requires a large variety of thorough investigations about model sensitivity and model ability to reproduce observed phenomena. Several aspects concerning model sensitivity and detailed diagnostic comparisons of simulated climate with observations have been discussed in the literature. Among recent works see for instance Boville (1991), Hayashi et al. (1989) and references therein.

Within the contest of the investigations aimed at validating comprehensive atmospheric models, the purpose of the present work is to examine the stratospheric performance of a modified version of the ECHAM3 (Roeckner et al., 1992) atmospheric general circulation model (GCM). The present

validation is based on a two year integration with monthly climatological forcing. The analysis of a 10 year integration is in progress and will be presented elsewhere.

The troposphere-stratosphere model used in this study is derived from a GCM with top in the middle stratosphere. It is therefore of interest to look at the impact of vertical resolution and location of the model top level on the simulation of the upper troposphere and lower stratosphere. This was done by considering annual mean forcing and integrating three versions of the GCM, with 35, 25 and 19 vertical levels respectively.

As far as comprehensive modelling of the stratosphere is concerned, there is now already some experience, the first attempt being the GFDL SKYHI model (Fels et al., 1980). More recently, several other groups have been involved in the development of middle atmosphere GCMs. For instance, the recent status of middle atmospheric modelling at NCAR is described in Boville (1991), the variability of the middle atmospheric model developed at GISS is described in Rind et al. (1988), and extensions of tropospheric GCMs to include the middle atmosphere are reported by Pawson et al. (1991) and Gray et al. (1993). An investigation about how equatorial planetary waves are affected by vertical resolution in the NCAR GCM has been performed by Boville and Randell (1992). Focused on detecting the sensitivity of the tropospheric circulation to the location of the model top level is the work of Boville and Cheng (1988).

The general circulation model used in the present work is described in Section 2. Results from the two year integration are reported in Section 3. A comparison of the simulated stationary planetary waves with observations compiled by the Freie Universität Berlin is also presented in section 3. Section 4 deals with the sensitivity to vertical resolution and the location of the model top level. Conclusions are drawn in Section 5.

2 THE MODEL

The atmospheric model used in this work is an upgraded version of the ECHAM3 general circulation model. A description of the numerical representation and physical parametrizations used in ECHAM3 is presented in Roeckner et al. (1992). The present-day climate as simulated by the ECHAM3 model and its earlier versions is also discussed in Roeckner et al. (1992). The main characteristics of ECHAM3 model are here briefly summarized. The model is a spectral GCM that can be integrated at various horizontal truncations (T21, T42, T63, and T106). The ECHAM3 standard vertical coordinate is a hybrid sigma-pressure coordinate with 19 vertical levels and the top at 10 hPa (hereafter L19). The modifications with respect to the ECHAM3 model included in this work are the following:

(i) A vertical coordinate with 35 vertical levels (hereafter L35) and the top at 0.1 hPa. This is

still a hybrid sigma-pressure coordinate with exactly the same vertical structure of ECHAM3 below 500 hPa. Above 500 hPa a finer resolution is used. In the construction of the L35 vertical structure, particular care was taken to ensure a smooth decrease in resolution with height and a resolution of about 1.5 km near the tropopause (compared to 2 km in ECHAM3). An additional vertical coordinate was also developed during the initial set up of the GCM. This latter vertical coordinate has 25 vertical levels (hereafter L25), the top at 0.3 hPa, and the same vertical structure of ECHAM3 below 50 hPa. The vertical structures of L19, L25, and L25 are shown in Figure 1.

(ii) A semi-Lagrangian transport scheme (Rasch and Williamson, 1990) for water vapor and cloud water. This scheme substitutes the previous Eulerian horizontal and vertical advection of cloud water and water vapor. With the introduction of the semi-Lagrangian transport, horizontal diffusion of could water and water vapor was also eliminated, while vertical diffusion was kept.

(iii) A radiation scheme (Morcrette, 1991) aimed at being flexible to the introduction of exotic trace gases and aerosols and at being able to take into account cloud-radiation interactions in considerable detail. This radiation scheme was further modified in the longwave radiative transfer calculation to take care of the Doppler broadening at low pressure following Fels (1979) and Schwarzkopf and Fels (1991), as described in Giorgetta and Morcrette (1993). In addition, the model - radiation scheme interface was slightly modified: Between full radiation time steps (the time interval during which the radiative transfer calculation is not updated) it is now assumed a constant net longwave radiative flux instead of the original constant effective emissivity. This change was motivated by a numerical instability arising at low pressure when the constant effective emissivity method was used. The source of such instability was traced down to be directly connected with the computation done between full radiation time steps by successfully integrating the GCM with the radiative transfer calculated at every time step. The diurnal cycle (included in ECHAM3) was excluded in all integrations reported to set the full radiation time step to 6 hours, instead of 2 hours (ECHAM3 standard), and therefore reducing the computational requirements.

(iv) A monthly zonal mean prescribed ozone distribution derived from a chemical model (Brühl, 1993) covering the troposphere-stratosphere-lower mesosphere. This distribution substitutes the original ECHAM3 ozone distribution, that was not designed for an atmospheric model extending above 10 hPa. Figure 2 shows the monthly zonal mean ozone distribution for January, April, July and October, on the vertical grid of the chemical model (MPIfC vertical grid).

(v) A $2d\nabla^4$ horizontal diffusion operator applied to divergence, vorticity, and temperature, with a slightly larger damping time for the latter two fields. The damping time reported is referred to a T21 truncation. In addition, a three-layer upper sponge for vorticity and divergence was introduced. The sponge coefficients from top are: $(1d)^{-1}$, $(4d)^{-1}$, $(16d)^{-1}$. The sponge layer is included in attempt

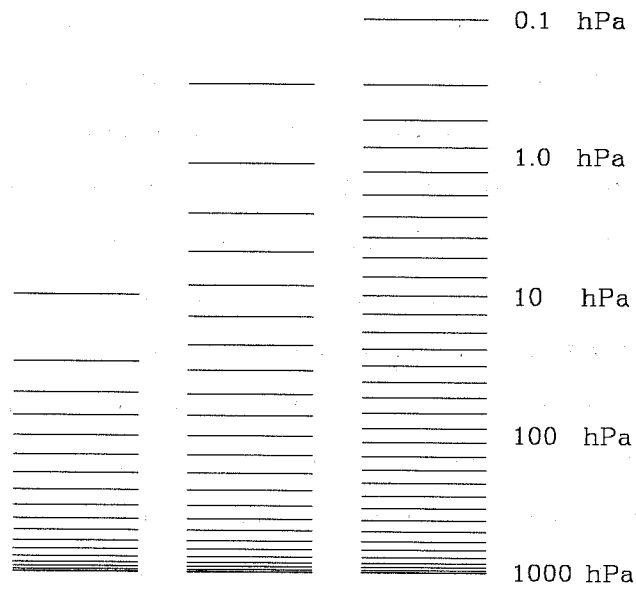

Fig 1 Comparison of L19, L25, and L35 vertical structures.

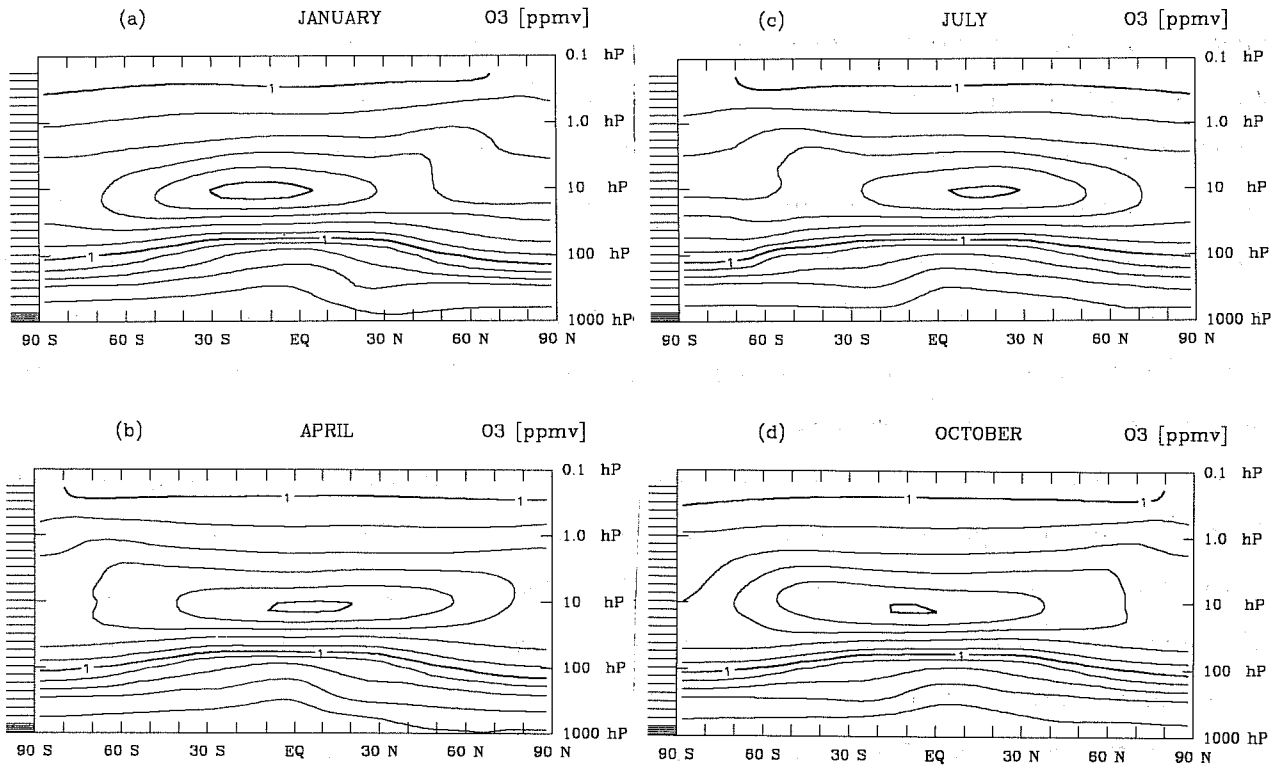

Fig 2 Monthly zonal mean ozone distribution used in the ECHAM simulation for (a) January, (b) April, (c) July and (d) October. Contours: 0.05, 0.1, 0.2, 0.5, 1, 2, 4, 6, 8, 10 ppmv. MPIfC vertical grid (courtesy of Ch. Brühl).

at reducing reflection from upward propagating waves. Both the horizontal diffusion and the upper sponge are not applied to the global mean, (0,0), and to waves (0,1) and (1,1).

Physical parametrizations as in ECHAM3: Prognostic scheme for stratiform clouds (Roeckner et al. 1991), cumulus convection parametrized by means of the Tiedtke (1989) mass flux scheme (including deep, midlevel and shallow convection), stratocumulus convection according to Tiedtke et al. (1988), a standard local vertical diffusion approach (Louis, 1979) revised to include cloud water effects (Roeckner, personal communication) and non-zero above the planetary boundary layer only for unstable stratification, planetary boundary layer according to Louis (1979), a five-layer model for heat conduction in soil and a refined bucket model for soil moisture (Blondin, 1989; Dümenil and Todini, 1992).

It is not the purpose of this work to investigate the impact on the GCM performance of modifications (ii) - (v). Modification (i) is discussed in Section 4.

3 THE TWO-YEAR SIMULATION

This section reports about the results of a two-year simulation performed with the GCM described above. T21 horizontal truncation and L35 vertical structure were used. Monthly climatological sea surface temperature were employed. The state of the atmosphere at January 1 of a previous integration was used as initial condition. The first two months were assumed to be sufficient as spinup and are excluded from the following discussion. The year label for each simulated year is the therefore defined to cover the period from March to the following February. Given that the modifications reported in Section 2 do not appear to dramatically alter the tropospheric circulation in the T21 version of the GCM, it is referred to Roeckner et al. (1992) for the basic characteristics of the tropospheric circulation.

3.1 Monthly zonal mean circulation

The monthly zonal mean wind and temperature for January and July of year one are presented in Figure 3. The respective year two fields are rather similar to that of year one and therefore not shown. The model levels drawn on the left side of each plot show that the upper sponge (top three levels) covers the lower mesosphere. Given that the sponge layer is introducing artificial tendencies, the model domain of interest is here limited to the troposphere and stratosphere. It is therefore natural to compare the GCM results with the observed climatology compiled by Randel (1992), hereafter R92. In R92 the general circulation statistics from twelve years (1979-1990) of National Meteorological Center (NMC) covering the atmosphere from 1000 to 1 hPa are reported. Although a monthly mean

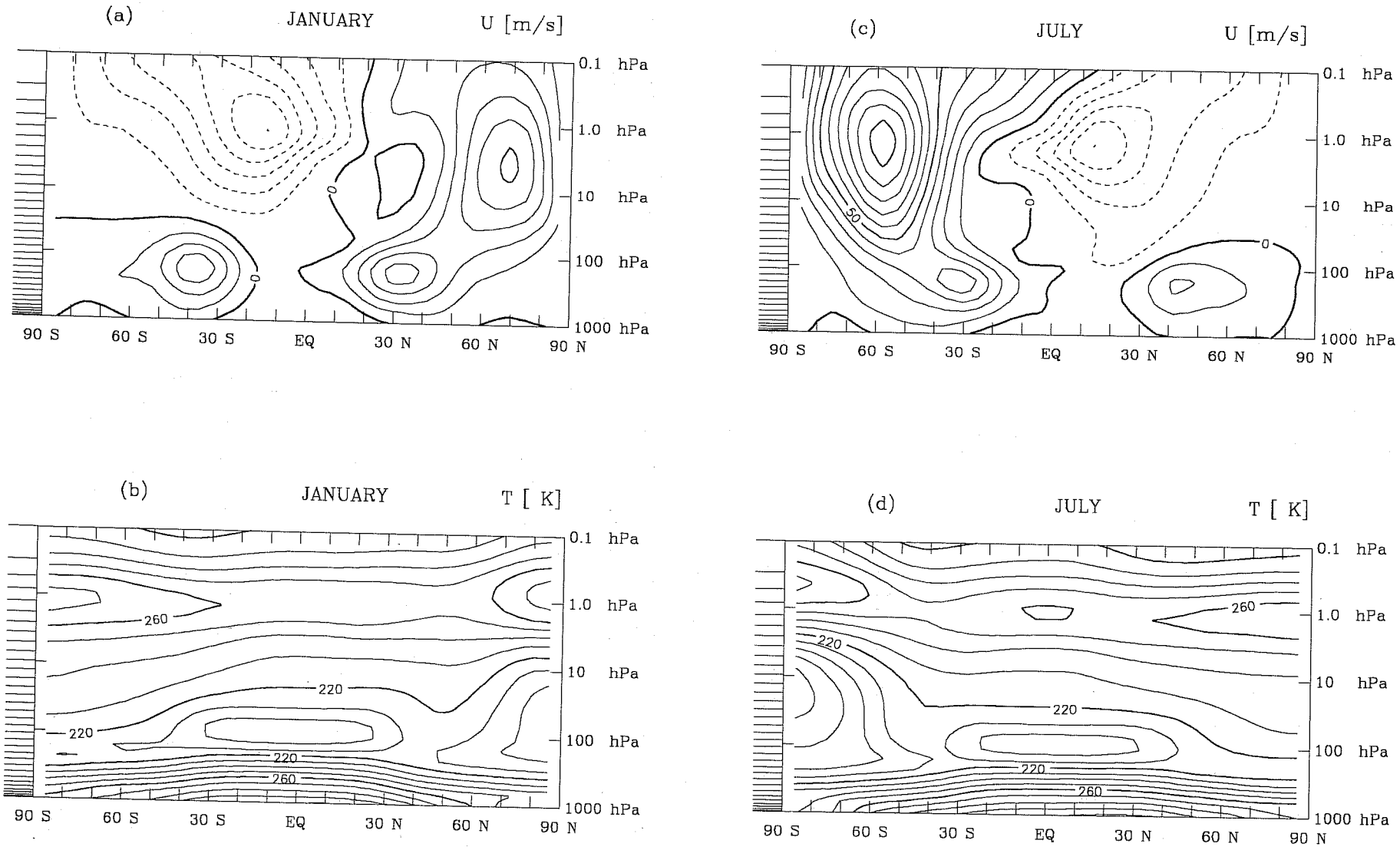

Fig 3 ECHAM simulation, year one: Monthly zonal mean wind for (a) January and (c) July, contour: 10 ms^{-1}; Monthly zonal mean temperature for (b) January and (d) July, contour: 10 ^{o}K.

from a two year integration cannot be directly compared with the observed climatology, in particular in regions of high interannual variability, insights about the model performance can be obtained by considering the simulated monthly mean as one realization of the samples included in computing a climatology. This kind of comparison is addressed in the following discussion of the results from the two year simulation.

In agreement with R92, Fig.3 (panel a and c) shows a clear separation between the polar stratospheric and subtropical tropospheric jets in the winter hemispheres as well as a clear confinement below 50 hPa of the subtropical tropospheric jets in the summer hemispheres. Another feature in agreement with observed monthly zonal mean winds is the asymmetry of the winter circulation in the stratosphere, the winter polar jet being generally stronger in the southern hemisphere than in the northern hemisphere. However, both winter polar stratospheric jet cores do not show the observed equatorward shift with height. This feature is seen also in January and July of year two (and in other winter months of both hemispheres), thus suggesting a systematic bias. Moreover, the winter hemisphere mean temperature (Fig.3, panel b and d) is characterized by a rather pronounced meridional gradient poleward of 50°-60° in the middle stratosphere and an overly cold (about 10^oK) minimum in the polar middle/lower stratosphere, even taking into account interannual variations. Such temperature minimum is also seen to extend too much into the middle latitudes in the lower stratosphere and upper troposphere of both winter hemispheres. Again, these features of the winter hemisphere mean temperature field are found also in January and July of year two as well as in other winter months of both hemispheres.

In the stratosphere, the magnitude of the zonal mean winds appears to be in reasonable agreement with R92 in both the winter and summer hemispheres. However, the easterly jet closes off in the lower instead than middle-high mesosphere, as generally observed (Barnett and Corney, 1985, a few year climatology derived from satellite data, over 1000-0.01 hPa). In the winter hemisphere, the altitude where the westerly stratospheric jet closes off is highly affected by interannual variations, preventing any definite conclusion from the simulation. It is reminded that in the upper stratosphere and lower mesosphere the GCM behavior depends crucially on the empoyment of the upper sponge, a better representation of this region may be obtained with a model domain extending up to 0.01 hPa (see for instance Hayashi et al. 1989).

In the summer stratosphere of both hemispheres the mean temperature (Fig.3, panel b and d) is in good agreement with R92 and also Barnett and Corney, (1985). The temperature maximum at about 1 hPa characterizing the stratopause is also clearly captured by the simulation. However, the magnitude of the temperature maximum at the summer pole at 1 hPa is about 10^oK less than observed, for both January and July. Given that the monthly interannual variability is rather low in

the summer season, this deficiency may be associated with either the presence of the sponge layer or with the exclusion of wavelength shorter than 0.2 μm in the radiative transfer calculation of the solar absorption (Morcrette, 1991).

The monthly zonal mean wind and temperature for April and October of year one are presented in Figure 4. In agreement with observations, Fig.4 shows that in April (panel a and b) the winter stratospheric vortex has already started to develop in the southern hemisphere and has basically disappeared in the northern hemisphere. In April year two (not shown) the monthly zonal mean wind is slightly stronger in the northern hemisphere stratosphere, thus suggesting a variability in the polar vortex breakdown. This topic will be addressed in more detail later in the discussion of the stationary planetary waves.

Fig.4 clearly shows that in October (panel c and d) the circulation in the southern hemisphere is still dominated by a rather strong polar vortex. While this feature is in qualitative agreement with observations, it seems that the breakdown of the southern hemisphere polar vortex occurs too slowly in the simulation. Moreover, the southern hemisphere mean wind in October year two (not shown) is rather similar to that of year one, suggesting that the model behavior is not much affected by internal variations (as it might actually be). In the boreal autumn the winter stratospheric vortex has already started to develop, in a similar way as during the austral autumn.

Finally, it is noted that in the vicinity of the equatorial stratopause Fig.3 and Fig.4 show easterly mean winds in January and July and westerly mean winds in April and October, suggesting a semi-annual oscillation in zonal wind maybe related to the observed one (Reed, 1966). From an inspection of the time development of the monthly zonal mean wind in the equatorial lower stratosphere there is instead no suggestions of the observed quasi-biennial oscillation in zonal wind (Reed et al., 1961) in the present two year simulation.

3.2 Stationary planetary waves

This section uses the observed monthly mean climatology compiled by the Freie Universität Berlin (FUB) and described in Pawson at al. (1993). The FUB climatology covers the northern hemisphere and includes temperature and geopotential height fields at 100, 50, 30 and 10 hPa. In the present work, the climatological monthly mean temperature and the standard deviation from the climatological monthly mean temperature for the winter months at 50 hPa (see Figure 5) and at 10 hPa (see Figure 7) are redrafted.

The northern hemisphere polar stereographic projection of the monthly mean temperature at 50 hPa, ECHAM simulation, is shown in Figure 6, for December (panel a and d), January (panel b and e) and February (panel c and f), year one at left and year two at right. A clear stationary wavenumber

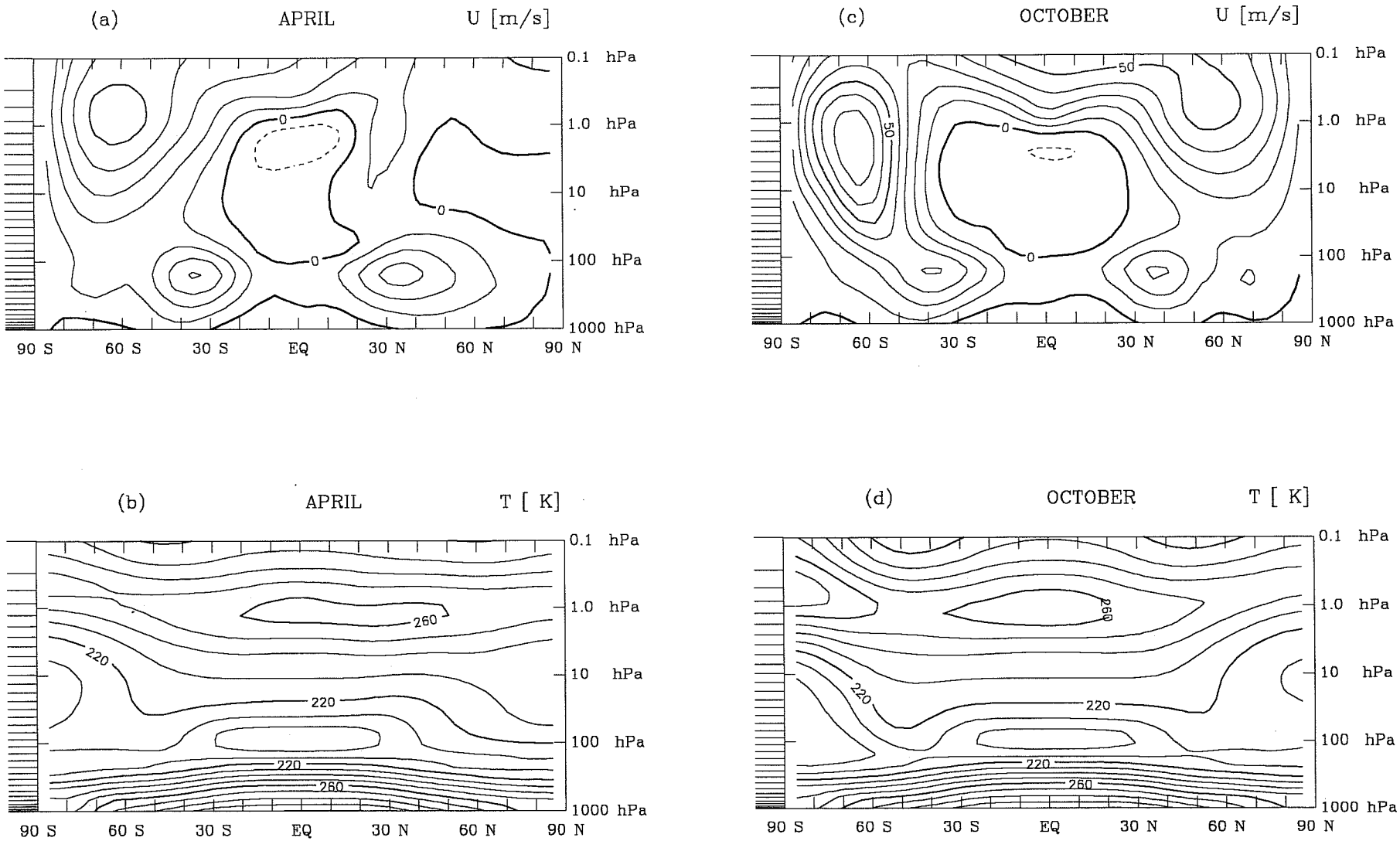

Fig 4 ECHAM simulation, year one: Monthly zonal mean wind for (a) April and (c) October, contour: 10 ms^{-1}; Monthly zonal mean temperature for (b) April and (d) October, contour: 10 ^{o}K.

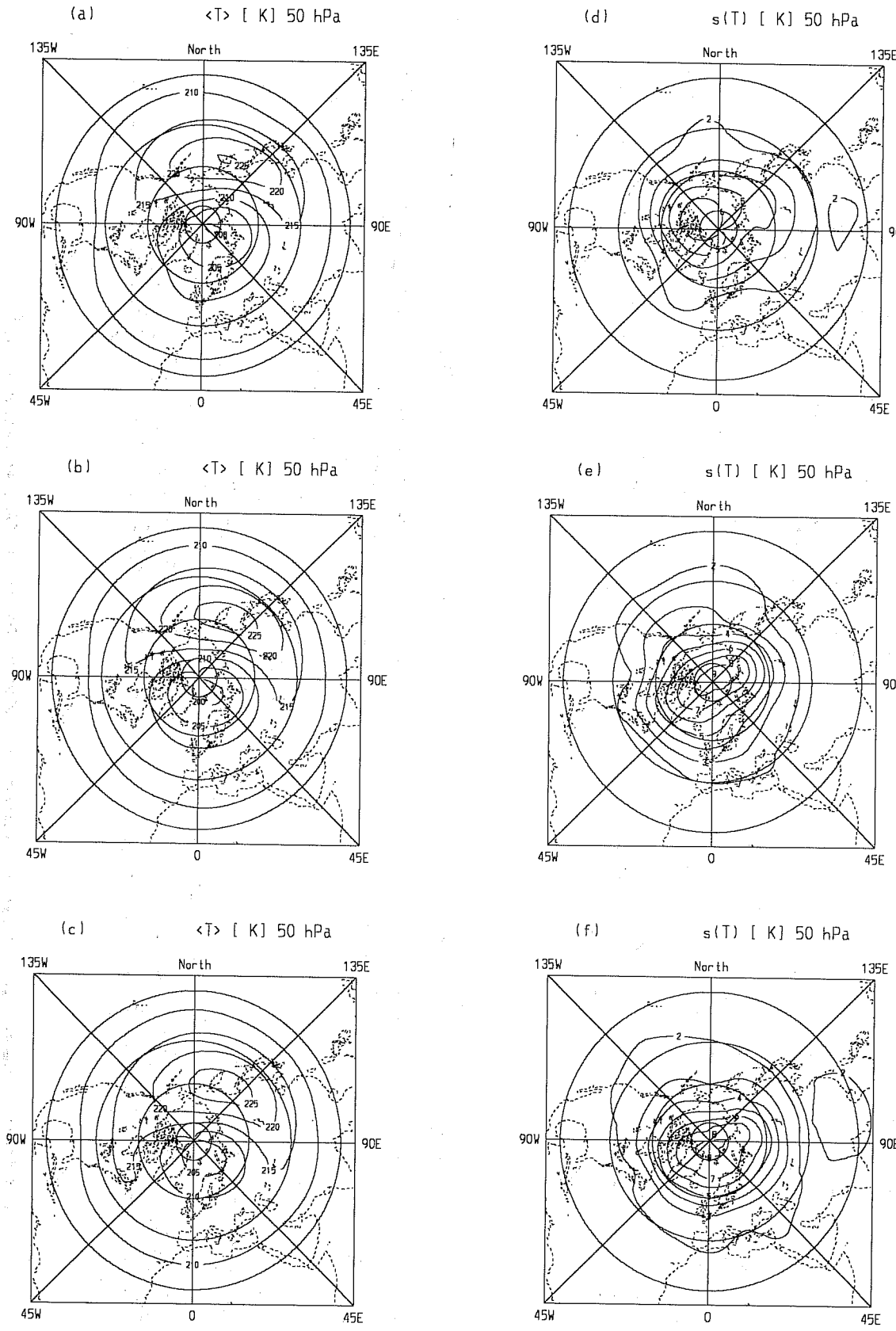

Fig 5 Northern hemisphere polar stereographic projection at 50 hPa, FU observations (1964-1992): Climatological monthly mean temperature for (a) December, (b) January and (c) February, contour: 5 °K; Standard deviation from the climatological monthly mean temperature for (d) December, (e) January and (f) February, contour: 1 °K. (Courtesy of S. Pawson).

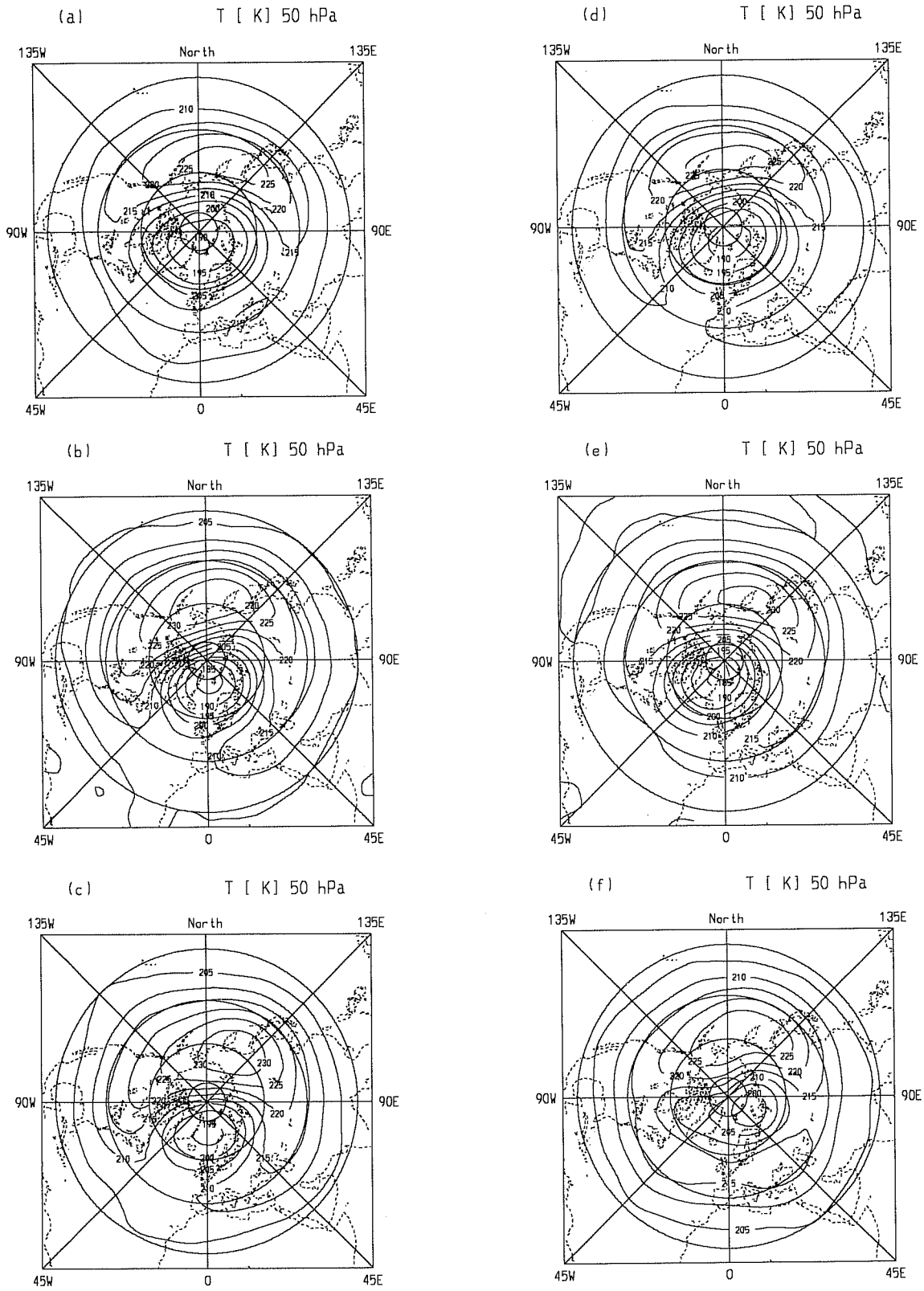

Fig 6 Northern hemisphere polar stereographic projection of the monthly mean temperature at 50 hPa, ECHAM simulation, year one at left and year two at right, for December, (a) and (d); January (b) and (e); and February, (c) and (f). Contour: 5 °K.

one pattern can be seen in all winter months of both years. In agreement with the FUB climatological monthly mean temperature, Fig.5, the simulated stationary wavenumber one is generally characterized by a temperature minimum with the center over Spitzbergen (poleward of northern Europe) and a temperature maximum in the North Pacific - Aleutian region.

The stationary wave amplitudes of the simulated winter seasons are remarkably similar in December (Fig.6, panel a and d): In both years the temperature maximum is about 225^oK and the temperature minimum is about 190^oK. While the temperature maximum could very well agree with the observed one, in both cases the temperature minimum is about 10^oK below the mean climatological value, in a region where the standard deviation is at most 4^o or 5^oK, see Fig.5 (panel a and d). These results suggest firstly that the interannual variability may be underestimated in the GCM and secondly that the temperature minimum is overly pronounced. The behavior of the stationary waves in January year one and two (Fig.6, panel b and e) is again characterized by a rather deep the temperature minimum. In February (Fig.6, panel c and f) the simulation is more satisfactory: Both the minimum and the maximum temperatures show a 5^oK variation, a value comparable to the observed standard deviation from climatology (Fig.5 panel c and f).

Figure 8 shows the corresponding northern hemisphere monthly mean temperature from the simulation at 10 hPa. Again, the comparison with the climatological mean and standard deviation (Fig.7) suggests a cold bias in the stationary wave minimum in early winter, especially in December (panel a and d). The cold bias appears to be present also during January of both years, although a slight variation in the location of the temperature minimum and a temperature difference of about 10^oK in the minimum are seen between January year one and January year two. However, a clear example of interannual variability is seen only in February (panel c and f), where in addition the stationary waves are not affected by the cold bias. It is interesting to note that the FUB standard deviations show a market increase of variability from December to January and February. This behavior appears to be qualitatively captured by the simulation.

The polar stereographic projection of the simulated monthly mean temperature for the austral winter stratosphere (not shown) indicates that in the GCM the circulation in the southern hemisphere is predominantly zonal, as expected from observations.

4 SENSITIVITY TO VERTICAL RESOLUTION

In this section, results from three integrations respectively with the L19, L25 and L35 vertical structures are reported. All three integrations were performed with annual mean conditions, i.e, annual mean insolation and annual mean distribution of ozone and sea surface temperature. A motionless

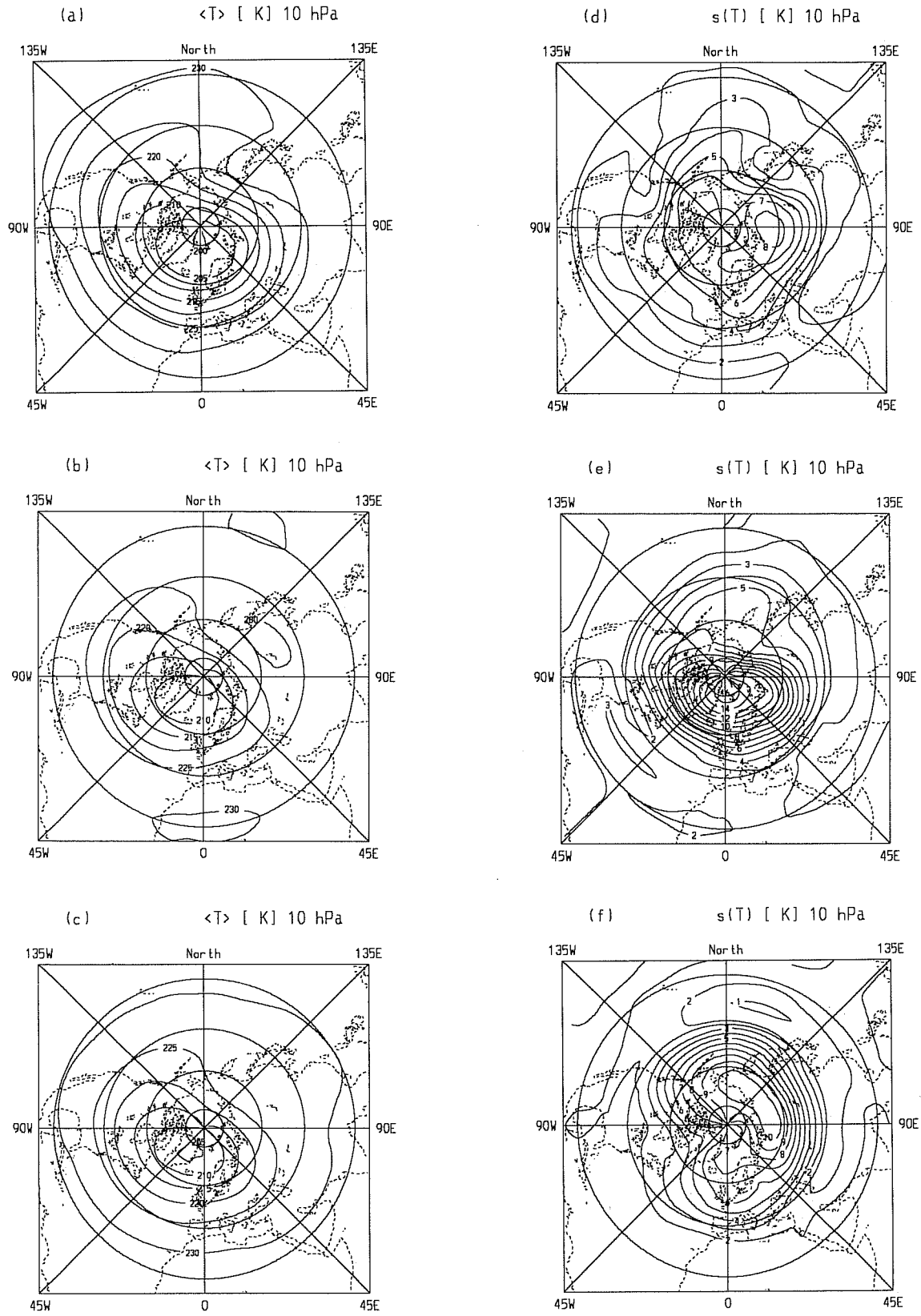

Fig 7 Northern hemisphere polar stereographic projection at 10 hPa, FU observations (1964-1971): Climatological monthly mean temperature for (a) December, (b) January and (c) February, contour: 5 °K; Standard deviation from the climatological monthly mean temperature for (d) December, (e) January and (f) February, contour: 1 °K. (Courtesy of S. Pawson).

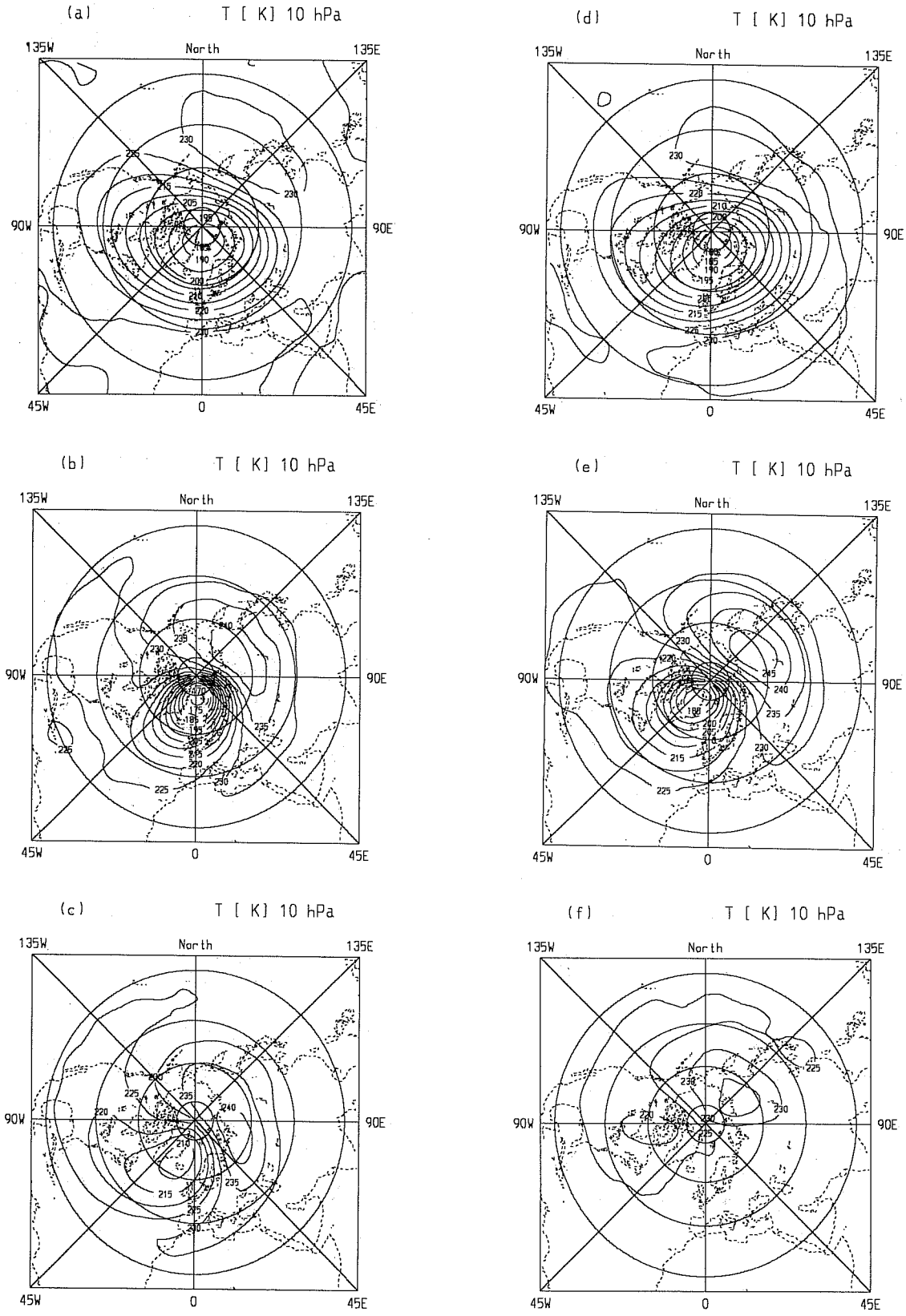

Fig 8 Northern hemisphere polar stereographic projection of the monthly mean temperature at 10 hPa, ECHAM simulation, year one at left and year two at right, for December, (a) and (d); January (b) and (e); and February, (c) and (f). Contour: 5 °K.

isothermal dry atmosphere was used as initial conditions in all cases. The first 240 days of the 600 day integration performed were assumed to be sufficient as spinup and are excluded from the discussion. This set of integrations was performed with an earlier version of the GCM described in Section 2. Namely, a version where in place of the upper sponge described in Section 2 the horizontal diffusion coefficient was increased (of a factor 60) in the top layer of the L25 and L35 models. This crude way to avoid spurious wave reflection at the model top is effective only for low order horizontal diffusion operators, in the following integrations a $2d\nabla^2$ was therefore used. In order to isolate the impact of vertical resolution and model top location, the coefficient of the horizontal diffusion operator was not enhanced at the top of the L19 model.

The 360-day average of the zonal mean wind for the three integrations is presented in Figure 9. The respective 360-day average of the zonal mean temperature is shown in Figure 10. In the stratosphere, westerly winds in both hemispheres are expected because of annual mean forcing. In the troposphere, the subtropical jets and temperature structure are virtually identical in the L19, L25 and L35 models. In the lower and middle stratosphere, it is straightforward notice distinct differences between the low top (L19) and the high top (L25 and L35) models: In both hemispheres, the L25 and L35 westerly zonal winds are about 10 ms^{-1} weaker than that in L19, and in the high top models the separation between the subtropical jets and the stratospheric jets is enhanced (Fig.9). Consistently, the L25 and L35 polar lower stratosphere is warmer (about 10^oK) than that of L19 (Fig.10). Given that the zonal mean wind and temperature simulated by L25 and L35 are in better agreement with those expected during the autumn season (see for instance R92), the changes undergoing in the lower-middle stratosphere of both hemispheres are considered to be an improvement.

Another interesting feature seen in Fig.9 is the closure of the stratospheric westerly jets in the lower mesosphere in the L35 simulation only. Moreover, the thermal structure of the stratopause is clearly defined only in the L35 simulation, see Fig.10. These two points indicate that the vertical structure of L35 model is better designed for the modelling of the troposphere-stratosphere system.

It is noted that in all versions and in both hemispheres the time evolution of the stratospheric polar vortex undergoes some vacillations in strength in the upper stratosphere and lower mesosphere. This is a very typical results in a GCM simulation forced by perpetual conditions (see for instance Boville, 1986).

The results presented here closely agree with that of Boville and Cheng (1988). In their work, Boville and Cheng (1988) compared two perpetual January simulations, one with a CGM with top level at 10 hPa and the other with top level at 0.1 hPa. In the northern hemisphere they found that the polar stratospheric jet was stronger and colder in the low top simulation. The use of annual mean forcing in the present work weakens the difference between the low and high top experiments (a difference of

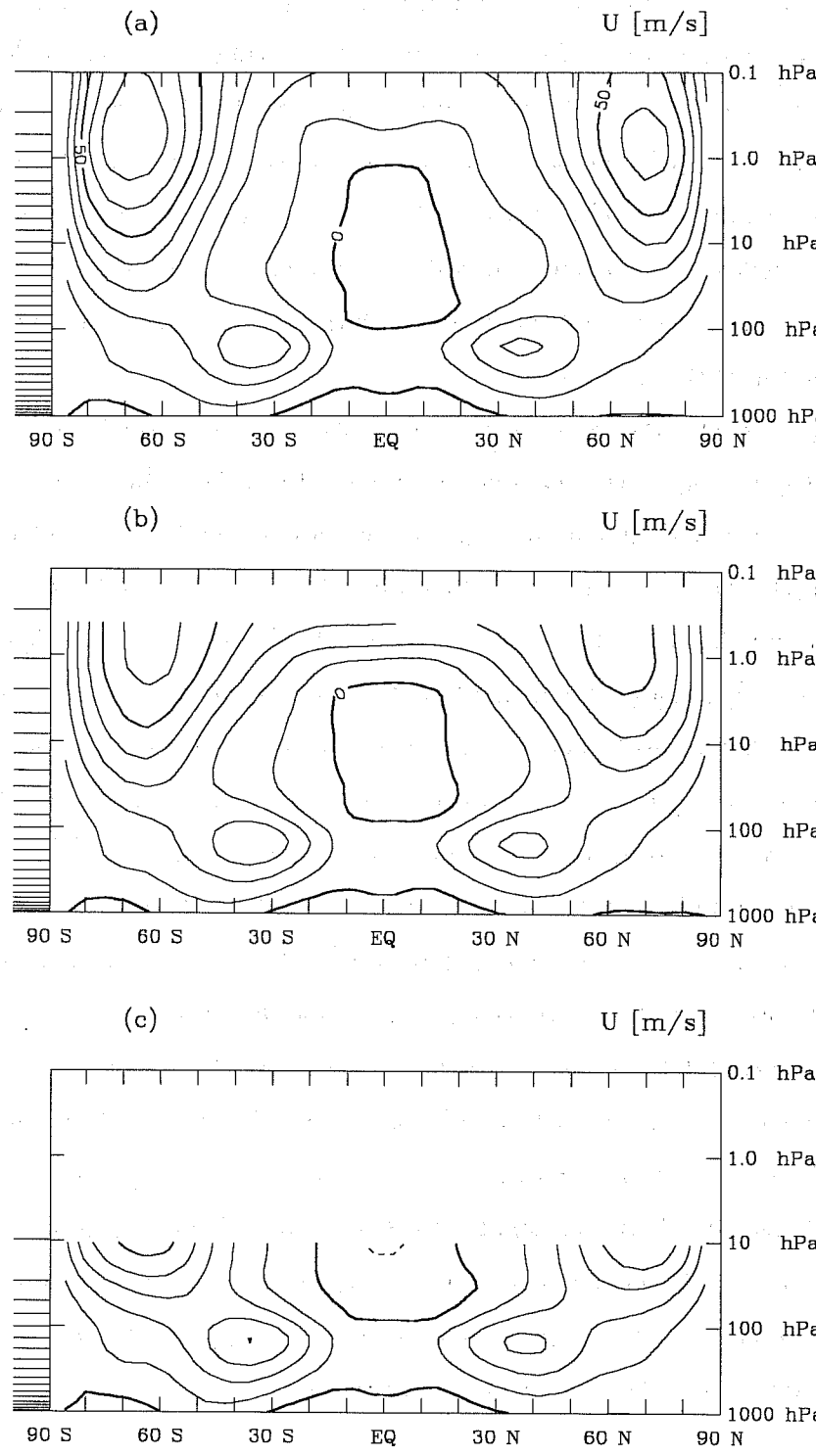

Fig 9 ECHAM integration with annual mean forcing: 360-day average of the zonal mean wind for (a) L35, (b) L25, and (c) L19, contour: 10 ms^{-1}.

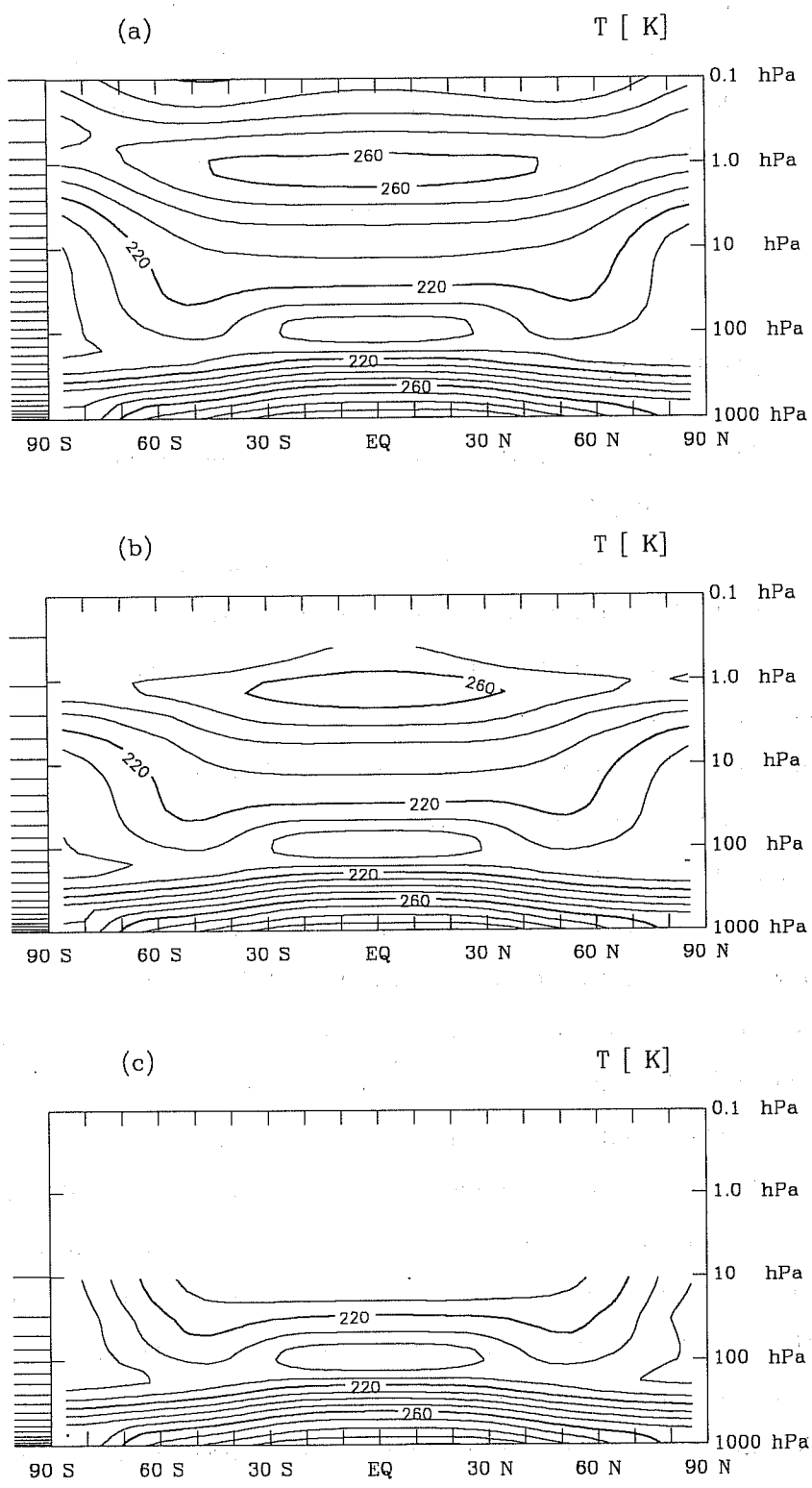

Fig 10 ECHAM integration with annual mean forcing: 360-day average of the zonal mean temperature for (a) L35, (b) L25, and (c) L19, contour: 10 ^{o} K.

about 30 ms^{-1} was indeed reported by Boville and Cheng, 1988 in the polar northern hemisphere), but in addition it has shown that the same result hold for the southern hemisphere. According to Boville and Cheng (1988), the cause of the changes in the lower polar stratospheric circulation is associated with planetary wave reflection in the low top GCM. Maybe a similar mechanism is responsible for the behavior found in L19. This question will be addressed by means of Eliassen-Palm diagnostic in a following study.

5 CONCLUSIONS

In this work the performance of the large scale circulation of the stratosphere simulated by a modified version of the ECHAM3 atmospheric general circulation model was examined. It was found that basic observed features are captured by the two-year seasonal cycle integration. The simulation is characterized by the typical annual change in the monthly zonal mean wind (westerly wind in winter and easterly wind in summer) in the stratosphere. A clear separation between the subtropical tropospheric jet and the polar stratospheric jet in winter and a clear confinement below 50 hPa of the subtropical tropospheric jet in summer have been found. In agreement with observations, the boreal winter circulation produced by the GCM is dominated by stationary planetary waves, while the austral winter circulation is predominantly zonal and is characterized by a stronger polar westerly wind jet. In the middle statosphere, the occurrence of late winter interannual variability in the stationary planetary wave amplitude was suggested. A preliminary inspection of the variability of a 10 year simulation (not shown) with the same GCM indicates indeed that in the middle and upper stratosphere the simulated variability is comparable to that observed (R92 and the FUB climatology).

Clear deficiencies of the winter simulation are an overly pronounced polar temperature minimum in the lower/middle stratosphere and the almost complete absence of the equatorward tilt with height of the westerly jet core. In the austral spring, the temperature bias may be responsible for the delay in the breakdown of the polar vortex. In the northern hemisphere lower stratosphere, the polar stereographic projections of the monthly mean temperature have shown that the excessive cold temperature in early winter is concurrent with insufficient interannual variability. An underestimation of the temperature variability in the lower stratosphere is also supported by the preliminary inspection of the variability of the 10 year simulation (not shown).

The cold bias in the polar stratospheric temperature is common to most of the existing middle atmosphere models. Given that the radiative equilibrium temperature in the winter hemisphere is much colder than the observed one (Fels, 1985), it is nowadays generally recognized that the cold bias occurring in GCMs is associated with insufficient dynamical forcing. As recently reviewed by McIntyre

(1992), such dynamical forcing is associated with the upward propagation of planetary and gravity waves generated in the troposphere. The planetary waves affect the circulation mainly in the lower stratosphere, while the impact on the general circulation of the gravity waves increases with elevation and predominates in the mesosphere. The role of the gravity waves in the lower stratosphere is a matter of current investigation. An improvement of the stratospheric simulation may therefore be achieved by a better representation of the dynamics and mechanical dissipation in the GCMs. However, the finest horizontal resolution that can be nowadays used in GCMs is probably not yet sufficient for the complete alleviation the systematic bias in temperature and zonal wind (see for instance Boville, 1991 and Hayashi et al. 1989). The impact of breaking gravity waves, for instance, would indeed require a thorough parametrization taking into account a variety of forcing mechanisms. These aspects will be investigated in subsequent developments of the ECHAM model.

Another deficiency of the present simulation appears to be a slightly weak stratopause summer temperature maximum associated with either the presence of the sponge layer or with inappropriate treatment of ultraviolet absorption in the solar radiation transfer calculation. About these points, it is planned to further extend the ECHAM model to 0.01 hPa and to revise the solar part of the radiation scheme.

Finally, the present model does not appear to produce any Quasi-Biennial Oscillation (QBO) of the zonal mean wind in the lower equatorial stratosphere, as virtually all GCMs simulations reported in the literature. A quasi-biennial signal at 10 hPa has been reported only by Cariolle et al. (1993). A recent discussion of the possible reasons for the difficulties related to the simulation of the QBO in GCMs can be found in Hamilton and Yuan (1992).

A first look at the impact of varying the location of the model top level and at the sensitivity to vertical resolution in the ECHAM model involved three annual mean integrations with: (1) the model top level at 0.1 hPa and 35 levels, (2) the model top level at 0.3 hPa and 25 levels, and (3) the model top level at 10 hPa and 19 levels, respectively. In agreement with Boville and Cheng (1988), it was found a weakening of the westerly winds and a warming in the polar lower stratosphere in both L25 and L35 in comparison with L19. Moreover, the L35 version was found to be better designed than the L25 version for the modelling of the troposphere-stratosphere system.

Acknowledgements

I wish to thank L. Bengtsson, J-J. Morcrette, and E. Roeckner for valuable discussions during the development of this work, Ch. Brühl for providing the ozone distribution, and S. Pawson for providing the FU climatology. I am also grateful to U. Schlese for helpful assistance about the GCM and K.

Arpe for reading this manuscript. The radiation scheme was implemented by M. Esch and U. Schlese and the semi-Lagrangian transport scheme by U. Hasson and U. Schlese.

References

Barnett, J. J., and M. Corney, 1985: Middle atmosphere reference model derived from satellite data. MAP Handbook, 16, 47-85.

Blondin, C., 1989: Research on land surface parameterization schemes at ECMWF. Proceedings of the workshop on "Parameterization of fluxes over land surface", ECMWF, Reading.

Boville, B. A., 1991: Sensitivity of simulated climate to model resolution. *J. Clim.*, 4, 469-485.

Boville, B. A., and X. Cheng, 1988: Upper boundary effects in a general circulation model. *J. Atmos. Sci.*, 45, 2591-2606.

Boville, B. A., and W. J. Randel, 1992: Equatorial waves in a stratospheric general circulation model; effect of vertical resolution. *J. Atmos. Sci.*, 49, 785-801.

Brühl, C., 1993: Atmospheric effects of stratospheric aircraft. Report of the 1992 models and measurements workshop. (Ed. M. Prather and E. Remsberg) NASA reference publication No 1292 II.

Cariolle, D., M. Amodei, M. Deque, J.F. Mahfouf, P.Simon, H. Teyssedre, 1993: A quasi-biennial signal in general circulation model simulations. *Science* , 261, 1313-1316.

Dümenil, L., and E. Todini, 1992: A rainfall-runoff scheme for use in the Hamburg climate model. Advances in theoretical hydrology, a tribute to James Dooge (Ed. J.P.O'Cane), EGS Series on Hydrological Sciences, 1, 129-157, Elsevier Press, 129-157.

Fels, S.B., 1976: Simple strategies for inclusion of Voigt effects in infrared cooling rate calculations. *App. Opt.*, 18, 2634-2637.

Fels, S.B., 1985: Radiative-dynamical interactions in the middle atmosphere. *Adv. Geophys.*, 28A, 277-300.

Fels, S. B., J. D. Mahlman, M. D. Schwarzkopf, and R. W. Sinclair, 1980: Stratospheric sensitivity to perturbations in ozone and carbon dioxide: radiative and dynamical response. *J. Atmos. Sci.*, 37, 2265-2297.

Giorgetta, M. and J.-J. Morcrette, 1993: Voigt line approximation in the ECMWF radiation scheme (in preparation).

Gray, L. J., M. Blackburn, M. P. Chipperfield, J. D. Haigh, D. Jackson, K. P. Shine, J. Thuburn, and W. Zhong, 1993: First Results from a 3-Dimensional Middle Atmosphere Model, *Adv. Space Res.*, 13, 1363-1372.

Hamilton, K. and L. Yuan, 1992: Experiments on tropical stratospheric mean-wind variations in a spectral general circulation model. *J. Atmos. Sci.*, 49, 2464-2483.

Hayashi, Y., D. G. Golder, J. D. Mahlman, and S. Miyahara, 1989: The effect of horizontal resolution on gravity waves simulated by the GFDL SKYHI general circulation model. *P. A. Geoph.*, 130, 421-443.

Louis, J.F., 1979: A parametric model of the vertical eddy fluxes in the atmosphere. *Boundary Layer Meteorology*, 17, 187-202.

McIntyre, M. E., 1992: Atmospheric dynamics: Some fundamentals, with observational implications. Proc. Int. School Phys. "Enrico Fermi" CXV Course *The use of EOS for studies of atmospheric physics* (Eds J. C. Gille and G. Visconti), North-Holland, pp 313-386.

Morcrette, J.J., 1991: Radiation and cloud radiative properties in the European Centre for Medium Range Weather Forecasts forecasting system. *J. Geophys. Res.*, 96, 9121-9132.

Pawson, S., K. Labitzke, R. Lenschow, B. Naujokat, B. Rajewski, M. Wiesner and R.-C. Wohlfart, 1993: Climatology of the northern hemisphere stratosphere derived from Berlin analyses. Part 1: Monthly means. *Meteorol. Abhandlung*, neue Folge Serie A, Band 7 Heft 4, Verlag von Dietrich Reimer, Berlin, G.

Pawson, S., U. Langematz, A. Mayer, P. Strauch, S. Leder, and K. Rose, 1991: A comparison of the climatology of a troposphere-stratosphere-mesosphere model with observations. *Cim. Dyn.*, 5, 161-174.

Randel, W. J., 1992: Global atmospheric circulation statistic, 1000-1 mb, *NCAR/TN-366+STR*, NCAR, Boulder, CO, USA.

Rasch, P. J., and D. L. Williamson, 1990: Computational aspect of moisture transport in global models of the atmosphere. *Quart. J. Roy. Meteor. Soc.*, 116, 1017-1090.

Reed, R. J., 1966: Zonal wind behavior in the equatorial stratosphere and lower mesosphere. *J. Geophys. Res.*, 71, 4223-4233.

Reed, R. J., W.J. Campbell, L. A. Rasmussen, and D. G. Rogers, 1961: Evidence of downward-propagating annual wind reversal in the equatorial stratosphere. *J. Geophys. Res.*, 66, 813-818.

Rind, D. R., R. Suozzo, and N. K. Balachandran, 1988: The GISS global climate middle atmosphere model. Part II: Model Variability due to interactions between planetary waves, the mean circulations, and gravity wave drag, *J. Atmos. Sci.*, 45, 371-386.

Roeckner, E., K. Arpe, L. Bengtsson, S. Brinkop, L. Dümenil, M. Esch, E. Kirk, F. Lunkeit, M. Ponater, B. Rockel, R. Sausen, U. Schlese, S. Schubert, W. Windelband, 1992: Simulation of the present-day climate with the ECHAM model: Impact of model physics and resolution. MPI Report. 93, 172 pp., Hamburg, G.

Roeckner, E., M. Rieland, and E. Keup, 1991: Modelling of cloud and radiation in the ECHAM model. ECMWF/WCRP Workshop on "Cloud, radiative transfer and the hydrological cycle", ECMWF, Reading, UK.

Schwarzkopf, M.D., and S. B. Fels, 1991: The simplified exchange method revisited: An accurate, rapid method for computation of infrared cooling rates and fluxes, *J. Geophys. Res.*, 96, 9075-9096.

Tiedtke, M., 1989: A comprehensive mass flux scheme for cumulus parametrization in large-scale models.*Mon. Wea. Rev.*, 117, 1779-1800.

Tiedtke, M., W. A. Heckley, and J. Slingo, 1988: Tropical forecasting at ECMWF: On the influence of physical parameterization on the mean structure of forecasts and analysis. *Quart. J. Roy. Meteor. Soc.*, 114, 639-664.